Eur. Phys. J. A **17**, 579–587 (2003)
DOI 10.1140/epja/i2003-10026-2

THE EUROPEAN PHYSICAL JOURNAL A

On a two-pomeron description of the F_2 structure function

A.I. Lengyel[1] and M.V.T. Machado[2,3,a]

[1] Institute of Electron Physics, National Academy of Sciences of Ukraine, Universitetska 21, UA-88016 Uzhgorod, Ukraine
[2] Instituto de Física e Matemática, Universidade Federal de Pelotas, Caixa Postal 354, CEP 96010-090, Pelotas, RS, Brazil
[3] High Energy Physics Phenomenology Group, GFPAE, IF-UFRGS, Caixa Postal 15051, CEP 91501-970, Porto Alegre, RS, Brazil

Received: 6 February 2003 / Revised version: 28 March 2003 /
Published online: 8 July 2003 –
Communicated by A. Schäfer

Abstract. We perform a global fit to the inclusive structure function considering a QCD-inspired model based on the summation of gluon ladders describing the *ep* scattering. In line with a two-pomeron approach, the structure function F_2 has a hard piece given by the model and the remaining soft contributions: the soft pomeron and non-singlet content. We have investigated several choices for the soft pomeron and its implication in the data description. In particular, we carefully estimated the relative role of the hard and the soft contributions in a large span of x and Q^2.

PACS. 13.60.Hb Total and inclusive cross-sections (including deep-inelastic processes) – 12.38.Bx Perturbative calculations – 12.40.Nn Regge theory, duality, absorptive/optical models

1 Introduction

A great challenge in understanding the hard interactions has been posed by the HERA small-x data [1] in order to describe the strong growth of the inclusive structure function F_2 as the Bjorken scale x decreases. This feature is also supplemented by the scaling violations on the hard scale given by the photon virtuality Q^2. The currently high accuracy reached turns out in the measurements having quite small statistic uncertainties, and probing a large interval of virtualities, *i.e.* from a real photon to thousands of GeVs. As far the Regge approach is concerned, at high energy the *ep* scattering process is dominated by the exchange of the pomeron trajectory in the t-channel. From the hadronic phenomenology, this implies that the structure function would present a mild increasing on energy ($s \simeq Q^2/x$), since the soft pomeron intercept ranges around $\alpha_{I\!P}(0) \approx 1.08$. Such behavior is in contrast with high-energy *ep* data, where the effective intercept takes the values $\lambda_{\rm eff} \simeq 1.3$–$1.4$. In the Regge language, this situation can be solved by introducing the idea of new poles in the complex angular-momentum plane, for instance rendered in the multipoles models [2–4], producing quite successful data description. Another proposition is given by the two-pomeron model [5], introducing an additional hard intercept and corresponding residue. However, a shortcoming from these approaches is the poor knowledge about the behavior on virtuality, in general modeled in an empirical way through the vertex functions. An interesting mixed procedure is to fix the initial conditions for the QCD parton distributions (valence and sea/gluon) in a sufficiently large initial scale $Q_0^2 \sim 1$–5 GeV^2 from the Regge phenomenology and then perform the QCD evolution up to higher virtualities [6,7].

On the other hand, the high photon virtuality allows the applicability of the QCD perturbative methods. Two main approaches emerge from the QCD formalism: the DGLAP and BFKL evolution schemes. The DGLAP formalism [8] is quite successful in describing most of the measurements on structure functions at HERA and hard processes in the hadronic colliders. This feature is even intriguing, since its theoretical limitations at high energy are well known [9]. The other perturbative approach is the BFKL formalism [10], well established at LO level but not yet completely understood at NLO accuracy. The main issue in the NLO BFKL effects is the correct account of the subleading corrections in the all-orders resummation [11] (for a pedagogical review, see, for instance, [12]). The LO BFKL approach can describe the HERA structure function in a limited kinematical range, *i.e.* at not so large Q^2 and small x. The main assumption at LO is that the processes described through the so-called hard pomeron are driven by gluon ladder diagrams with infinite rungs of s-channel gluons at asymptotic energies. A consistent treatment considering higher-order resummations is currently in progress and should be available soon. An open issue is whether the available energies in the nowadays

[a] e-mail: magnus@if.ufrgs.br

colliders actually are asymptotic, allowing the use of the complete BFKL series.

In this work we perform a global data fitting to the HERA structure function F_2 using as a model for the hard pomeron the finite sum of gluon ladders [13]. The model is based on the truncation of the BFKL series keeping only the first few orders in the strong-coupling perturbative expansion, where subleading contributions can be absorbed in the adjustable parameters. From the phenomenology on hadronic collisions [14], just three orders, $\sim (\alpha_s \ln(1/x))^2$, are enough to describe current accelerator data. The hard-pomeron model should be supplemented by a soft piece accounting for the non-perturbative contributions to the process. The description, therefore, turns out similar to the two-pomeron model [5], with the advantage of a complete knowledge of the behavior on x and Q^2. Concerning the energy dependence, the hard piece has the logarithmic growth in contrast with the effective powerlike behavior on the model [5]. The original model contains a reduced number of adjustable parameters: the normalization $\mathcal{N}_p$ and the non-perturbative scale μ^2 from the proton impact factor and the parameter x_0 scaling the logarithms on energy. More details on those parameters are addressed in the next section. In a previous study in ref. [15], two distinct choices for the soft pomeron were analyzed. The resulting two-pomeron model was successful in describing data on the structure function F_2 and its derivatives (slopes on Q^2 and x) for $x \leq 2.5 \cdot 10^{-2}$ and $0.045 \leq Q^2 \leq 1500$ GeV^2. Here, we extend the kinematical range of fitting and the models considered for the soft pomeron.

This paper is organized as follows. In the next section, we shortly review the main expressions for the hard piece given by the summation up to the two-rung ladder contribution. In sect. 3, an overall fit to the recent deep inelastic data is performed based on the hard contribution referred above supplemented by the remaining soft pomeron and non-singlet contributions. The role played by the hard and soft contributions are investigated in detail. There, we also draw up our conclusions.

2 The hard contribution: summing gluon ladders

In this section, we review the elements needed to compute the structure function using the finite sum of gluon ladders in the ep collision, with the photon-proton center-of-mass energy labeled by W. Before that, let us shortly motivate the picture of the finite sum of gluon ladders. At finite energies, the LLA and NLLA summation implies that the amplitude is represented by a finite sum on terms, where the number of terms increases like $\ln s$, rather than by the solution of the BFKL integral equation. The interest in taking the firts terms in the complete series in the truncation is related to the fact that the energies reached by the present accelators are not high enough to accommodate a big number of gluons in the ladder rungs that eventually hadronize. In the energy range of HERA there can be only a few real gluons produced in any scattering event. On the other hand, in the LO BFKL resummation real gluons can be emitted without any cost in energy, while in reality the production of a real gluon requires an energy equivalent to one or one and a half units of rapidity. This violation of energy conservation is probably cured in the NLO BFKL resummation or by relying on consistency constraint implementing energy conservation in numerical simulations of LO BFKL evolution. The truncation of the whole series could be similar to this consistency condition. Corroborating the truncation hypothesis, for example the coefficient weighting the term $\sim \ln^3 s$, turns out to be compatible with zero considering even the Tevatron data [14], in contrast with those expected from the complete resummation.

The proton inclusive structure function, written in terms of the cross-sections for the scattering of transverse or longitudinal polarized photons, reads as [16]

$$F_2(x,Q^2) = \frac{Q^2}{4\pi^2\alpha_{\rm em}} \left[\sigma_T(x,Q^2) + \sigma_L(x,Q^2)\right] , \qquad (1)$$

$$\sigma_{T,\,L}(x,Q^2) = \frac{\mathcal{G}}{(2\pi)^4} \times \int \frac{{\rm d}^2\boldsymbol{k}}{\boldsymbol{k}^2} \frac{{\rm d}^2\boldsymbol{k}'}{\boldsymbol{k}'^2} \, \Phi^{\gamma^*}_{T,\,L}(\boldsymbol{k}) \, \mathcal{K}(x,\boldsymbol{k},\boldsymbol{k}') \, \Phi_p(\boldsymbol{k}') \, , \qquad (2)$$

where $\mathcal{G}$ is the color factor for the color singlet exchange and $\boldsymbol{k}$ and $\boldsymbol{k}'$ are the transverse momenta of the exchanged Reggeized gluons in the t-channel. The $\Phi^{\gamma^*}_{T,\,L}(\boldsymbol{k})$ is the virtual-photon impact factor and $\Phi_p(\boldsymbol{k}')$ is the proton impact factor. The first one is well known in perturbation theory at leading order, while the latter is modeled since in the proton vertex there is no hard scale to allow pQCD calculations. The kernel $\mathcal{K}(x,\boldsymbol{k},\boldsymbol{k}')$ contains the dynamics of the process, for instance, the BFKL kernel.

The amplitudes can be calculated order by order: for instance, the Born contribution coming from the two-gluon exchange and the one-rung ladder contribution read as

$$\mathcal{A}^{(0)} = \frac{2\,\alpha_s\,W^2}{\pi^2} \sum_f e_f^2 \int \frac{{\rm d}^2\boldsymbol{k}}{\boldsymbol{k}^4} \, \Phi^{\gamma^*}_{T,\,L}(\boldsymbol{k}) \, \Phi_p(\boldsymbol{k}) \, ,$$

$$\mathcal{A}^{(1)} = \frac{6\alpha_s^2 W^2}{8\pi^4} \sum_f e_f^2 \, \ln\left(\frac{W^2}{W_0^2}\right) \times \int \frac{{\rm d}^2\boldsymbol{k}}{\boldsymbol{k}^4} \frac{{\rm d}^2\boldsymbol{k}'}{\boldsymbol{k}'^4} \, \Phi^{\gamma^*}_{T,\,L}(\boldsymbol{k}) \, \mathcal{K}(\boldsymbol{k},\boldsymbol{k}') \, \Phi_p(\boldsymbol{k}') \, ,$$

where α_s is considered fixed since we are in the framework of the LO BFKL approach. The perturbative kernel $\mathcal{K}(\boldsymbol{k},\boldsymbol{k}')$ can be calculated order by order in the perturbative expansion [16]. The pomeron is attached to the off-shell incoming photon through the quark loop diagrams, where the Reggeized gluons are attached to the same and to different quarks in the loop. The virtual-photon impact factor averaged over the transverse polarizations reads as [17,18]

$$\Phi^{\gamma^*}_{T,\,L}(\boldsymbol{k}) = \frac{1}{2} \int_0^1 \frac{{\rm d}\tau}{2\pi} \int_0^1 \frac{{\rm d}\rho}{2\pi} \, \frac{\boldsymbol{k}^2(1-2\,\tau\,\tau')(1-2\,\rho\,\rho')}{\boldsymbol{k}^2\,\rho\,\rho' + Q^2\rho\,\tau\,\tau'} , \qquad (3)$$

where ρ, τ are the Sudakov variables associated with the momenta in the photon vertex and $\tau' \equiv (1-\tau)$ and $\rho' \equiv (1-\rho)$.

Gauge invariance requires the proton impact factor vanishing at $\boldsymbol{k}'$ going to zero and is modeled in a simple way,

$$\Phi_p(\boldsymbol{k}') = \mathcal{N}_p \, \frac{\boldsymbol{k}'^2}{\boldsymbol{k}'^2 + \mu^2}, \tag{4}$$

where $\mathcal{N}_p$ is the unknown normalization of the proton impact factor and μ^2 is a scale which is typical of the non-perturbative dynamics. These scales will be considered adjustable parameters in the analysis. Considering the electroproduction process, summing the first orders in perturbation theory we can write the expression for the inclusive structure function,

$$F_2^{\rm hard}(x,Q^2) = \frac{8}{3}\,\frac{\alpha_s^2}{\pi^2}\sum_f e_f^2\,\mathcal{N}_p \times \left[I^{\,(0)}(Q^2,\mu^2) + \frac{3\,\alpha_s}{\pi}\,\ln\frac{x_0}{x}\,I^{\,(1)}(Q^2,\mu^2) + \frac{1}{2}\left(\frac{3\,\alpha_s}{\pi}\,\ln\frac{x_0}{x}\right)^2 I^{\,(2)}(Q^2,\mu^2)\right], \tag{5}$$

where the functions $I^{\,(n)}(Q^2,\mu^2)$ correspond to the n-rung gluon ladder contribution. The quantity x_0 gives the scale normalizing the logarithms on energy for the LLA BFKL approach, which is arbitrary and enters as an additional parameter. The contributions are written explicitly as

$$I^{\,(0)} = \frac{1}{2}\ln^2\left(\frac{Q^2}{\mu^2}\right) + \frac{7}{6}\ln\left(\frac{Q^2}{\mu^2}\right) + \frac{77}{18}\,, \tag{6}$$

$$I^{\,(1)} = \frac{1}{6}\ln^3\left(\frac{Q^2}{\mu^2}\right) + \frac{7}{12}\ln^2\left(\frac{Q^2}{\mu^2}\right) + \frac{77}{18}\ln\left(\frac{Q^2}{\mu^2}\right) + \frac{131}{27} + 2\,\zeta(3)\,, \tag{7}$$

$$I^{\,(2)} = \frac{1}{24}\ln^4\left(\frac{Q^2}{\mu^2}\right) + \frac{7}{36}\ln^3\left(\frac{Q^2}{\mu^2}\right) + \frac{77}{36}\ln^2\left(\frac{Q^2}{\mu^2}\right) + \left(\frac{131}{27} + 4\zeta(3)\right)\ln\left(\frac{Q^2}{\mu^2}\right) + \frac{1396}{81} - \frac{\pi^4}{15} + \frac{14}{3}\zeta(3)\,, \tag{8}$$

where $\zeta(3) \approx 1.202$. The clear behavior on x and virtuality is worth mentioning. The main result in ref. [15] is in good agreement, in terms of a χ^2/dof test, for the inclusive structure function in the range $0.045 \le Q^2 \le 1500$ GeV^2, once considered the restricted kinematical constraint $x \le 0.025$. The non-perturbative contribution (from the soft dynamics), initially considered as a background, was found to be not negligible. In the next section, we perform a global analysis, extending the range on x fitted by adding the non-singlet contribution modeled through the usual Regge parameterizations and analyzing also the multipole models for the soft pomeron.

3 Fitting results and conclusions

In order to perform the fitting procedure, for the hard piece one uses eq. (5) and for the soft piece we have selected some typical models, as addressed below. First, one takes into account the latest version [19] of the CKMT model [20], having an economical number of parameters,

$$F_2^{\rm soft}(x,Q^2) = A\left(\frac{1}{x}\right)^{\Delta(Q^2)} \times \left(\frac{Q^2}{Q^2+a}\right)^{\Delta(Q^2)+1}(1-x)^{n_s(Q^2)}\,, \tag{9}$$

$$\Delta(Q^2) = \Delta_0\left(1 + \frac{Q^2\Delta_1}{\Delta_2+Q^2}\right),$$

$$n_s(Q^2) = \frac{7}{2}\left(1 + \frac{Q^2}{Q^2+b}\right), \tag{10}$$

where $\Delta(Q^2)$ is the pomeron intercept. The non-singlet term takes the following form:

$$F^{ns}(x,Q^2) = A_R\,x^{1-\alpha_R}\left(\frac{Q^2}{Q^2+a_R}\right)^{\alpha_R}(1-x)^{n_{ns}(Q^2)}, \tag{11}$$

$$n_{ns}(Q^2) = \frac{3}{2}\left(1 + \frac{Q^2}{Q^2+d}\right). \tag{12}$$

The CKMT model was originally constructed to interpolate between the soft hadronic pomeron phenomenology, where $\alpha_{\rm pom} \simeq 1.08$, and the growth for the low-Q^2 proton structure function in deep inelastic scattering, where $\alpha_{\rm pom} \simeq 1.2$. This is obtained through absorbtive corrections to the bare soft pomeron, leading to a Q^2-dependent intercept. Therefore, in phenomenological application considering a two-pomeron approach, we should be careful in verifying the soft pomeron intercept coming out.

Another possibility is to select a soft piece which corresponds to the pomeron with intercept equal to unity and has the form of non-perturbative truncated $\ln\left(\frac{Q^2}{x}\right)$ series (soft multipole pomeron) [3,4], given by

$$F_2^{\rm soft}(x,Q^2) = Q^2\left[A\cdot\left(\frac{a}{Q^2+a}\right)^{\alpha} + B\cdot\ln\left(\frac{Q^2}{x}\right)\left(\frac{a}{Q^2+a}\right)^{\beta}\right] \tag{13}$$

for the dipole pomeron and

$$F_2^{\rm soft}(x,Q^2) = Q^2\left[A\cdot\left(\frac{a}{Q^2+a}\right)^{\alpha} + B\cdot\ln^2\left(\frac{Q^2}{x}\right)\left(\frac{a}{Q^2+a}\right)^{\beta}\right] \tag{14}$$

for the tripole pomeron.

Table 1. Parameters of the fit. Procedure (I): hard + soft terms; procedure (II): similar to analysis (I), but restricting soft pomeron intercept; procedure (III): only hard term and non-singlet contribution. Procedure (IV): hard + soft dipole pomeron terms; procedure (V): hard + soft tripole pomeron terms.

		(I)	(II)	(III)		(IV)	(V)
	$\mathcal{N}$	0.0237	0.0238	0.0195		0.0269	0.0195
Hard pomeron	μ^2	1.36	1.40	0.108		1.42	1.33
	x_0	$0.798 \cdot 10^{-2}$	$1.01 \cdot 10^{-2}$	$0.398 \cdot 10^{-2}$		$0.833 \cdot 10^{-2}$	$0.808 \cdot 10^{-2}$
	α_s	0.202	0.217	0.0804		0.204	0.215
	A	0.327	0.366	–	A	0.291	0.220
	a	0.754	1.11	–	a	2.39	1.19
Soft pomeron	Δ_0	$0.638 \cdot 10^{-2}$	0.07(fixed)	–	α	1.87	1.32
	Δ_1	25.7	6.00	–	B	$0.712 \cdot 10^{-2}$	$0.437 \cdot 10^{-3}$
	Δ_2	6.31	0.02(fixed)	–	β	1.20	1.17
	b	33.4	7.35	2.00		19.6	39.5
	A_R	5.94	6.73	10.3		6.31	5.88
Non-singlet	a_R	653	306	869		502	650
	d	1.14	0.796	2.22		0.947	1.02
χ^2/dof		1.10	1.23	1.39		1.09	1.03

The multipole means the soft pomeron is considered as multiple poles instead of just a single pole. This approach has been successful in hadron-hadron and lepton-hadron (mostly vector meson photoproduction) scattering, where the increase of the cross-section on energy can be produced with a unit pomeron intercept. The multipole model has shown to be quite stable in fitting simultaneously hadronic and lepton-hadron data.

Concerning the hard piece, eq. (5), we selected the overall normalization factor as a free parameter, defined as $\mathcal{N} = \frac{8}{3}\frac{\alpha_s^2}{\pi^2}\sum e_f^2 \mathcal{N}_p$, considering four active flavors. That contribution was also supplemented by a factor $(1-x)^{n_s}$ accounting for the large-x effects. The remaining parameters are the scales μ^2 and x_0 as well as the coupling constant α_s (considered at a fixed scale in the BFKL formalism). As we will see in the following, its value presents a small variation in the fitting, suggesting that it can be considered fixed as $\alpha_s = 0.2$, which is typical in the HERA kinematical region.

For the fitting procedure we consider the data set containing all available HERA data for the proton structure function F_2 [21–30] updated with a new HERA experiment [31] and adding only the latest (E665 and NMC) data set of fixed-target experiments [32,33]. This choice for the selection of data sets follows the procedures used in ref. [3]. The whole data set contains a total number of 1059 experimental points, covering the complete available x and virtualities $0.045 \leq Q^2 \leq 30000$ GeV^2. It should be stressed that the inclusion of the older fixed-target experimental data (SLAC [34] and BCDMS [35]) requires a more sophisticated study for the background, for example, following the ALLM parameterization or as in ref. [3]. However, for that purpose the number of free parameters would be significantly larger.

Here, we have considered the following distinct fitting procedures:

- (I) Overall fit considering the hard piece and the CKMT soft pomeron plus reggeon piece, eqs. (9) and (11).
- (II) Overall fit restricting the soft pomeron intercept, modifying the expression for $\Delta(Q^2)$, see eq. (10), in the CKMT soft pomeron. It reads now as

$$\Delta(Q^2) = \Delta_0 \left(\frac{Q^2}{\Delta_1 + Q^2} \right) + \Delta_2 \,. \qquad (15)$$

- (III) The fit is performed considering only the hard piece plus the non-singlet contribution.
- (IV) and (V) Overall fit using the hard pomeron piece and the soft multipoles pomeron, eqs. (13) and (14). The main feature is the soft pomeron having an intercept equal to unity.

The best-fit parameters for these procedures are presented in table 1. The kinematical range covered is $0 \leq x \leq 1$ and $0.045 \leq Q^2 \leq 30000$. In the following we discuss each procedure, pointing out the relative contribution from the hard and soft pieces and its quality.

Let us start from procedure (I). The parameters for the hard piece remain consistent with the previous analysis in [15], *i.e.* $\alpha_s \sim 0.2$, $x_0 \simeq 10^{-2}$ and μ^2 of order 1 GeV^2. Concerning the soft pomeron, the bare intercept Δ_0 comes out quite small in the whole range of Q^2. This fact seems to corroborate a soft pomeron having an intercept close to unity in this two-pomeron analysis. The same happens for procedure (II), with a modified form for the CKMT intercept. For low Q^2, the intercept comes out small, but at higher virtualities reaches the upper limit $\Delta = 0.08$.

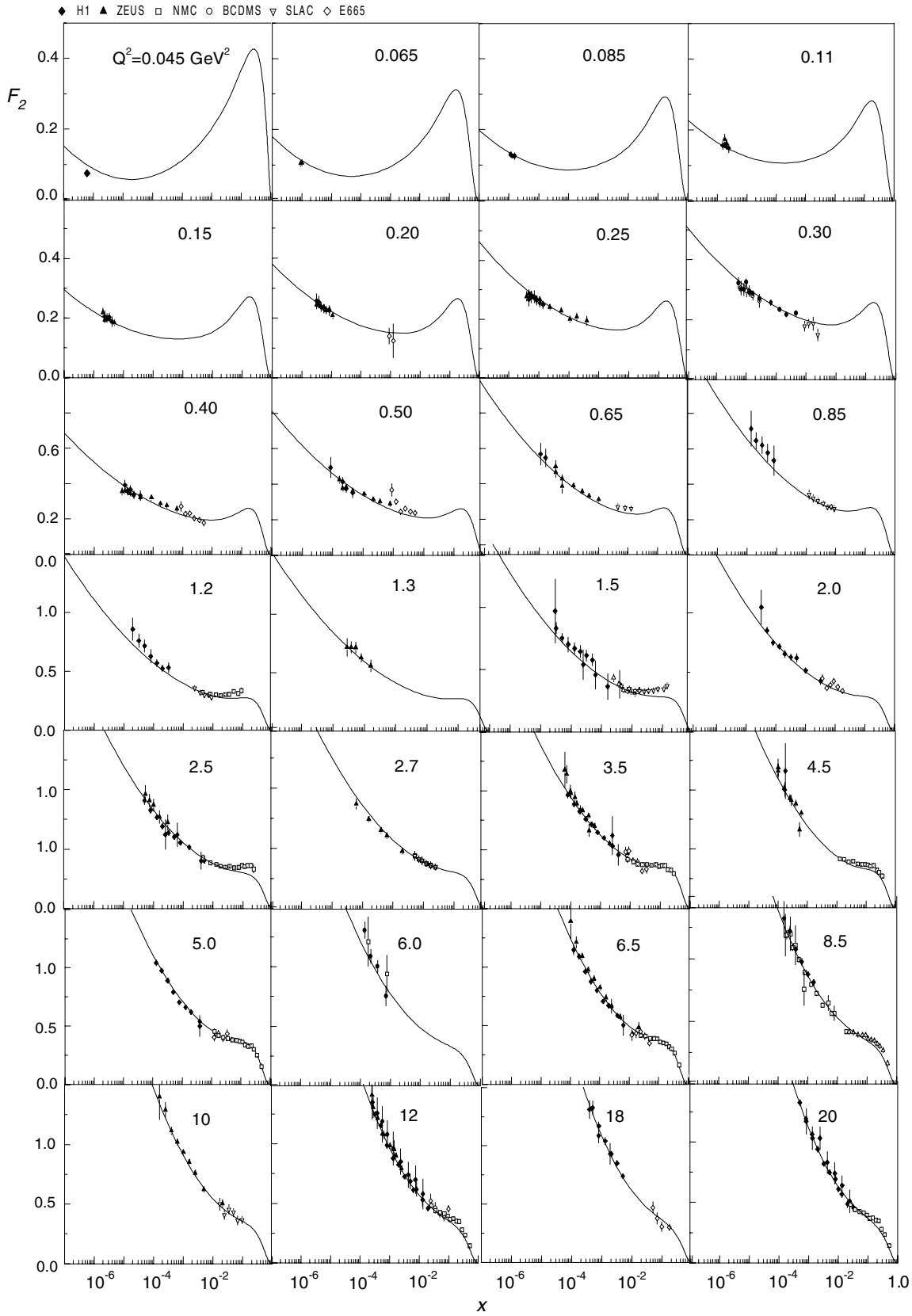

Fig. 1. The inclusive structure function at small-Q^2 virtualities. The procedures (I)-(V) produce nearly equivalent curves. The SLAC [34] and BCDMS [35] data are not included into the fit. The virtualities are in units of GeV^2.

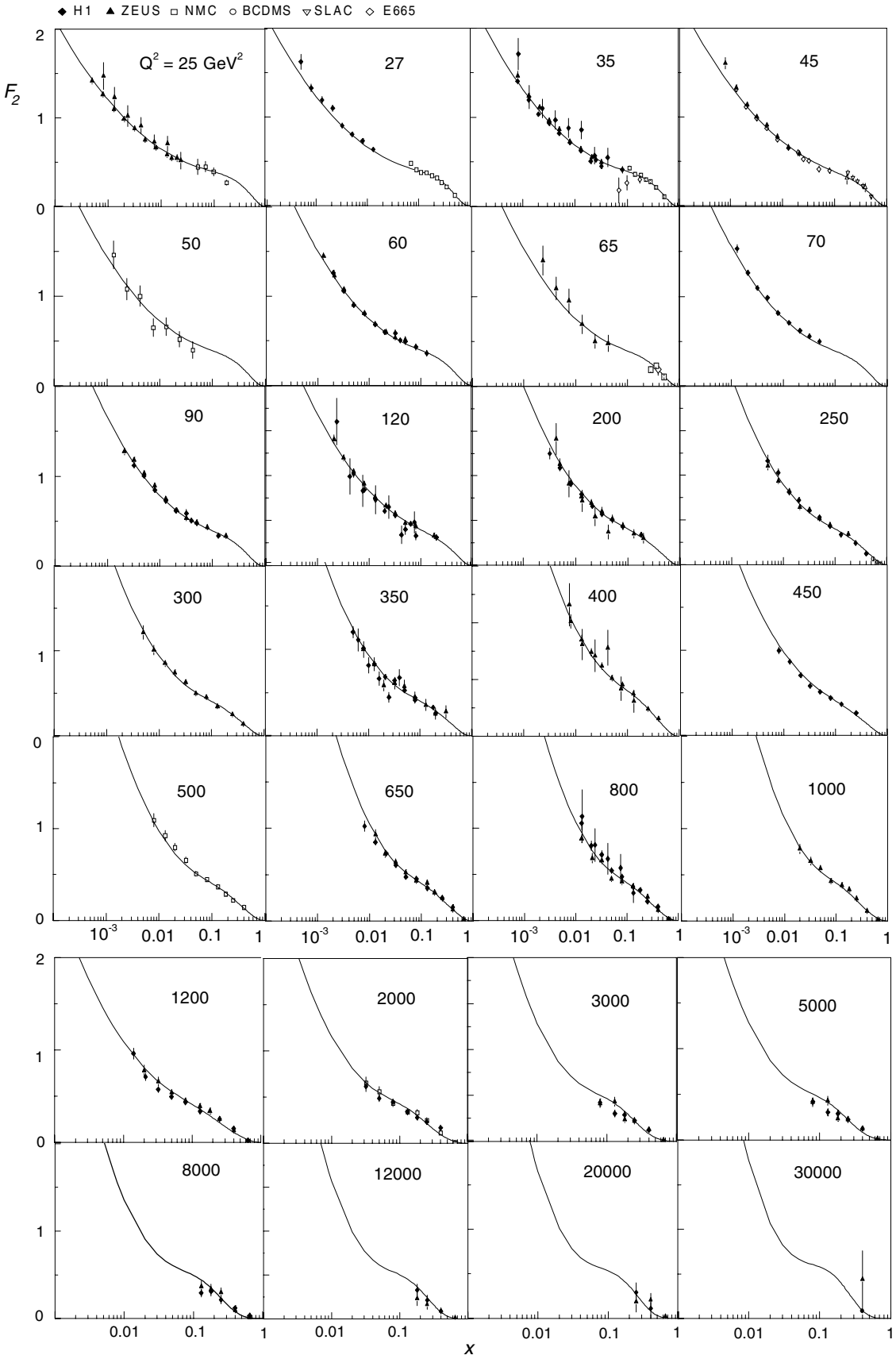

Fig. 2. The results for the inclusive structure function at medium- and high-Q^2 virtualities (in units of GeV^2).

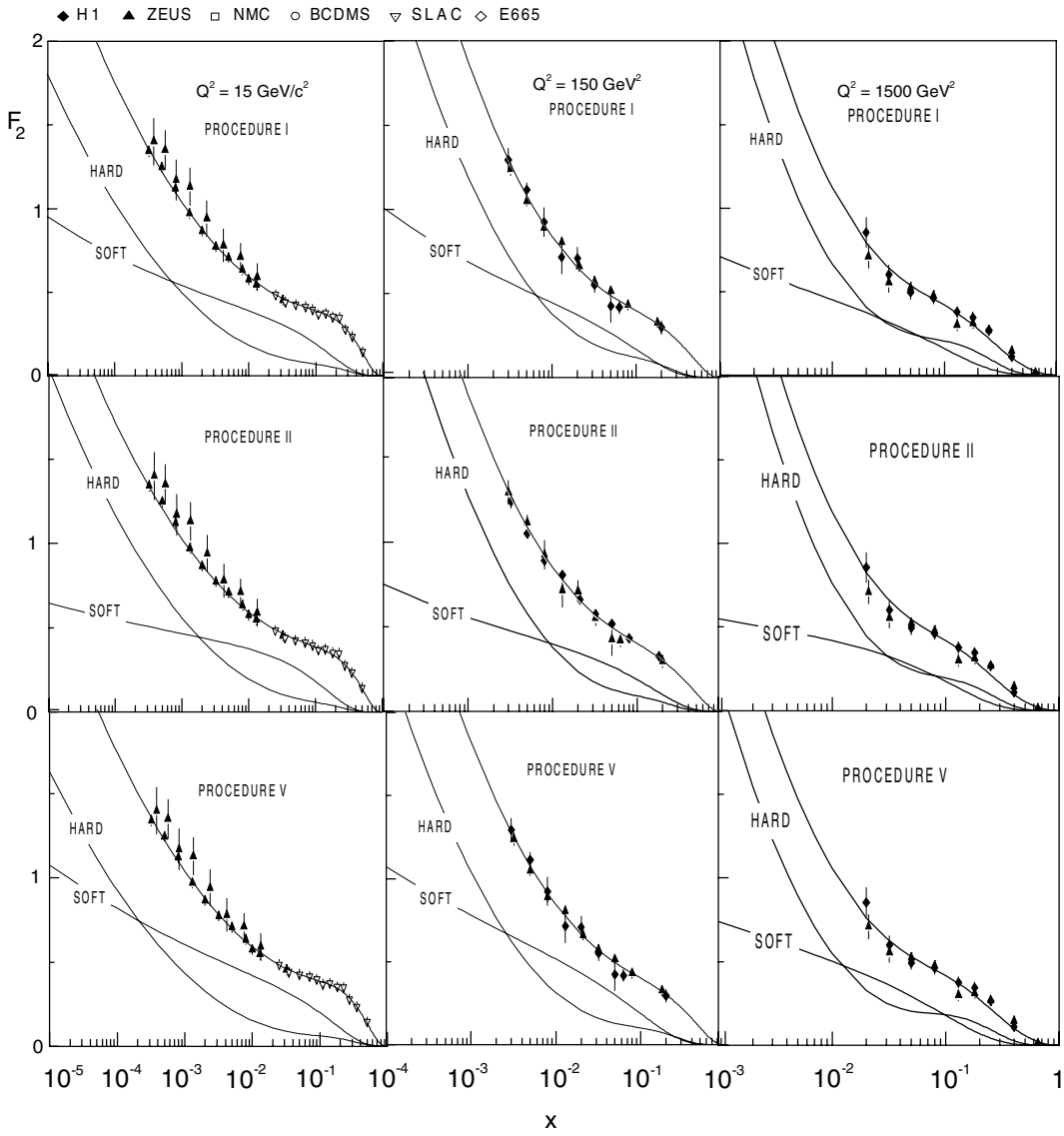

Fig. 3. The results for the inclusive structure function at $Q^2 = 15$, 150 and 1500 GeV^2 virtualities with the contribution of soft and hard pieces for the different procedures.

Procedures (IV) and (V), considering the soft multipole pomeron, provide the best quality of fit $\chi^2/\text{dof} \simeq 1$. The tripole pomeron is preferred as a soft background, giving a slightly better result than the dipole pomeron. Concerning the hard piece, the value for the fixed coupling constant is quite stable, $\alpha_s \simeq 0.2$, consistent with the overall HERA value.

The situation differs only in procedure (III), where a small value for α_s is found, suggesting, in this case, that the best choice would be $\alpha_s = 0.119$, which coincides with $\alpha_s(M_Z)$. The high χ^2/dof for this case is not quite sizeable, in view of the smaller number of parameters considered (8 against 13 from the remaining analysis).

In figs. 1 and 2, we present the fit result for the inclusive structure function for small and large virtualities. The plots for the different procedures lie on top of each other. In fig. 3, we present the relative role of the distinct contributions for the fit. The hard and soft pieces are presented separately. We present them explicitly for the virtualities 15, 150 and 1500 GeV^2, where the contributions from fitting (I), (II) and (V) are shown. It is verified that the region where the hard pomeron starts to dominate depends on the vituality. For instance, at $Q^2 = 15$ GeV^2 it stays on $x \sim 10^{-3}$ for the different procedures, whereas it is shifted to $x \sim 10^{-2}$ at $Q^2 = 1500$ GeV^2. A two-pomeron picture is supported, comparable with those using the two-pomeron analysis in refs. [3,5].

Additionally, we performed the fit restricting the domain of the Bjorken variable to $x \leq 0.07$. This procedure is similar to that considered in the analysis of ref. [3]. For this purpose, we restricted the number of free parameters (equal to 10) for the soft + hard pomeron model, as in the Donnachie-Landshoff model reanalysis considered in [3]. To this aim, we fixed the constant $\alpha_s = 0.2$ as well as the

Table 2. Parameters of the fit for restricted domain $x \leq 0.07$. Procedure (A): hard + soft terms; procedure (B): hard + soft dipole pomeron terms; procedure (C): hard + soft tripole pomeron terms.

		(A)		(B)	(C)
	$\mathcal{N}$	0.0196		0.0280	0.0195
Hard pomeron	μ^2	1.38		1.42	0.143
	x_0	$0.915 \cdot 10^{-2}$		$0.793 \cdot 10^{-2}$	$0.940 \cdot 10^{-2}$
	A	0.317		0.134	0.212
	a	0.757		2.74	1.25
Soft pomeron	Δ_0	0.0515	α	2.18	1.39
	Δ_1	3.38	B	$0.469 \cdot 10^{-2}$	$0.513 \cdot 10^{-3}$
	Δ_2	9.27	β	1.20	1.19
	A_R	10.2		10.4	10.2
Non-singlet	a_R	698		112	543
χ^2/dof		0.95		1.00	0.92

powers $n_s = 7$ and $n_{ns} = 3$. The following procedures were considered: (A) hard + soft terms; (B) hard + soft dipole pomeron terms; (C) hard + soft tripole pomeron terms. Results of the fit are presented in table 2. The quality of our approach is similar to those found in ref. [3], at least in this specific domain, $x \leq 0.07$. The parameters for the multipole pomeron seem stable in this kinematical region. There is a change in case (A), where the bare pomeron intercept is higher than in procedure (I) producing a usual soft result $\Delta \simeq 0.08$. The parameters for the hard piece remain stable in all fitting procedures.

In conclusion, we verify that the fitting procedure is equivalent to the model using the two-pomeron approach [3,5], with the advantage of the clear understanding of the behaviors on x and Q^2 of the corresponding hard content. In particular, the behavior on Q^2 of the hard piece sheds light on further implementations of the hard pomeron residue in the two-pomeron fitting. The fitting procedure shows that the soft pomeron has an intercept smaller than the usual $\alpha_{I\!P} = 1.08$, suggesting that a suitable choice is the multipole pomeron having intercept equal to unity. In particular, the tripole pomeron presented the best-fit result in all kinematical ranges considered here, followed by the dipole one. The fitting using only the hard piece and the non-singlet contributions is not completely ruled out, producing a not so high χ^2/dof result.

M.V.T.M. thanks the support of the High Energy Physics Phenomenology Group (GFPAE, IF-UFRGS) at Institute of Physics, Porto Alegre.

References

1. M. Klein, Int. J. Mod. Phys. A **15S1**, 467 (2000).
2. P. Desgrolard, A. Lengyel, E. Martynov, Eur. Phys. J. C **7**, 655 (1999); P. Desgrolard, L. Jenkovszky, F. Paccanoni, Eur. Phys. J. C **7**, 263 (1999).
3. P. Desgrolard, E. Martynov, Eur. Phys. J. C **22**, 479 (2001).
4. J.R. Cudell, G. Soyez, Phys. Lett. B **516**, 77 (2001).
5. A. Donnachie, P.V. Landshoff, Phys. Lett. B **518**, 63 (2001) and references therein.
6. L. Csernai, L. Jenkovszky, K. Kontros, A. Lengyel, V. Magas, F. Paccanoni, Eur. Phys. J. C **24**, 205 (2002).
7. G. Soyez, e-Print Archive: hep-ph/0211361.
8. Yu.L. Dokshitzer, Sov. Phys. JETP **46**, 641 (1977); G. Altarelli, G. Parisi, Nucl. Phys. B **126**, 298 (1977); V.N. Gribov, L.N. Lipatov, Sov. J. Nucl. Phys. **28**, 822 (1978).
9. A.H. Mueller, Phys. Lett. B **396**, 251 (1997).
10. E.A. Kuraev, L.N. Lipatov, V.S. Fadin, Phys. Lett B **60**, 50 (1975); Sov. Phys. JETP **44**, 443 (1976); **45**, 199 (1977); Ya. Balitsky, L.N. Lipatov, Sov. J. Nucl. Phys. **28**, 822 (1978).
11. V.S. Fadin, L.N. Lipatov, Phys. Lett. B **429**, 127 (1998); M. Ciafaloni, G. Camici, Phys. Lett. B **430**, 349 (1998).
12. G.P. Salam, Acta Phys. Pol. B **30**, 3679 (1999).
13. M.B. Gay Ducati, M.V.T. Machado, Phys. Rev. D **63**, 094018 (2001); Nucl. Phys. (Proc. Suppl.) B **99**, 265 (2001); e-Print Archive: hep-ph/0104192.
14. R. Fiore *et al.*, Phys. Rev. D **63**, 056010 (2001).
15. M.B. Gay Ducati, K. Kontros, A. Lengyel, M.V.T. Machado, Phys. Lett. B **533**, 43 (2002).
16. V. Barone, E. Predazzi, *High Energy Particle Diffraction* (Springer-Verlag, Heidelberg, 2002).
17. E.M. Levin, M.G. Ryskin, Sov. J. Nucl. Phys. **53**, 653 (1991).
18. Ya. Balitsky, E. Kuchina, Phys. Rev. D **62**, 074004 (2000).
19. A.B. Kaidalov, C. Merino, D. Pertermann, Eur. Phys. J. C **20**, 301 (2001).
20. A. Capella, A.B. Kaidalov, C. Merino, J. Tran Thanh Van, Phys. Lett. B **337**, 358 (1994).
21. H1 Collaboration (T. Ahmed *et al.*), Nucl. Phys. B **439**, 471 (1995).
22. H1 Collaboration (S. Aid *et al.*), Nucl. Phys. B **470**, 3 (1996).
23. H1 Collaboration (C. Adloff *et al.*), Nucl. Phys. B **497**, 3 (1997).

24. H1 Collaboration (C. Adloff *et al.*), Eur. Phys. J. C **13**, 609 (2000).
25. H1 Collaboration (C. Adloff *et al.*), Eur. Phys. J. C **21**, 33 (2001).
26. H1 Collaboration (C. Adloff *et al.*), Phys. Lett. B **520**, 183 (2001).
27. ZEUS Collaboration (M. Derrick *et al.*), Z. Phys. C **72**, 399 (1996).
28. ZEUS Collaboration (J. Breitweg *et al.*), Phys. Lett. B **407**, 432 (1997).
29. ZEUS Collaboration (J. Breitweg *et al.*), Eur. Phys. J. C **7**, 609 (1999).
30. ZEUS Collaboration (J. Breitweg *et al.*), Nucl. Phys. B **487**, 53 (2000).
31. ZEUS Collaboration (S. Chekanov *et al.*), Eur. Phys. J. C **21**, 443 (2001).
32. E665 Collaboration (M.R. Adams *et al.*), Phys. Rev.D **54**, 3006 (1996).
33. NMC Collaboration (M. Arneodo *et al.*), Nucl. Phys. B **483**, 3 (1997).
34. SLAC old experiments (L.W. Whitlow *et al.*), Phys. Lett. B **282**, 475 (1992).
35. BCDSM Collaboration (A Benvenuti *et al.*), Phys. Lett. B **223**, 485 (1989).